Anomalous Effect of Flow Rate on the Electrochemical Behavior at a Liquid|Liquid Interface under Microfluidic Conditions

ARTICLE *in* LANGMUIR · DECEMBER 2013

Impact Factor: 4.46 · DOI: 10.1021/la403614z · Source: PubMed

6 AUTHORS, INCLUDING:

Wojciech Adamiak
Polish Academy of Sciences
14 PUBLICATIONS **42** CITATIONS
SEE PROFILE

Tomasz Kalwarczyk
Instytut Chemii Fizycznej PAN
26 PUBLICATIONS **262** CITATIONS
SEE PROFILE

Krzysztof Sozański
Instytut Chemii Fizycznej PAN
13 PUBLICATIONS **44** CITATIONS
SEE PROFILE

Martin Jönsson-Niedziolka
Polish Academy of Sciences
52 PUBLICATIONS **520** CITATIONS
SEE PROFILE

Langmuir

Article

pubs.acs.org/Langmuir

Anomalous Effect of Flow Rate on the Electrochemical Behavior at a Liquid|Liquid Interface under Microfluidic Conditions

Dawid Kaluza, Wojciech Adamiak, Tomasz Kalwarczyk, Krzysztof Sozanski, Marcin Opallo, and Martin Jönsson-Niedziolka*

Institute of Physical Chemistry, Polish Academy of Sciences, Kasprzaka 44/52, 01-224 Warsaw, Poland

Supporting Information

ABSTRACT: We have investigated the oxidation of ferrocene at a flowing organic solvent|aqueous electrolyte|solid electrode junction in a microfluidic setup using cyclic voltammetry and fluorescent laser scanning confocal microscopy. At low flow rates the oxidation current decreases with increasing flow, contrary to the Levich equation, but at higher flow rates the current increases linearly with the cube root of the flow rate. This behavior is explained using a simple model postulating a smallest effective width of the three-phase junction, which after fitting to the data comes to be ca. 20 μm. The fluorescence microscopy reveals mixing of the two phases close to the PDMS cover, but the liquid|liquid junction is stable close to the glass support. This study shows the importance of the solid|liquid|liquid junctions for the behavior of multiphase systems under microfluidic conditions.

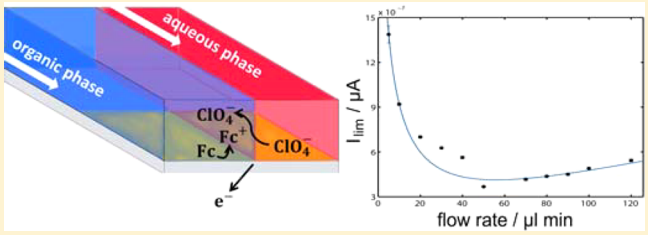

INTRODUCTION

Microfluidics offers electrochemistry an increased mass transport rate in comparison to typical stagnant conditions. This gives an enhanced current response, greater sensitivity, and reproducibility. Microfluidic systems can be therefore advantageous from the analytical applications point of view, for example in construction of microfluidic amperometric sensors. Hydrodynamic conditions in electrochemistry are typically achieved by using large rotating disk macroelectrodes or flow injection systems.[1] Microfluidics is more advantageous for that purpose, as it operates with smaller volumes of reagents and it allows microelectrodes to be fabricated whose geometry can be precisely controlled during the photolithographic procedure.[2]

Microfluidics has been successively applied to chemistry,[3,4] biology,[5,6] and electrochemistry.[7,8] Electrochemical microfluidic systems have been used as electrochemical reactors in fuel cells,[9,10] in analytical chemistry as sensors,[11,12] and in preparative electrosynthesis.[13,14] Microfluidic voltammetry in the presence and absence of electrokinetic flow has been addressed in numerous reports (see for example refs 15−19). For the sake of our work it is important to highlight the report by Fisher et al.[17] The authors found that under single phase flow conditions limiting current is proportional to the cube root of the flow rate. The authors showed for the first time that this relationship, which was developed for larger channels, is applicable also to microfluidic channels under single phase flow conditions.

In the case of multiphase flow, where two liquid phases flow parallel to each other along the central channel, a liquid|liquid interface exists. When such interface is present, electrode reactions are coupled to ion transfer processes across the interface. Under stationary conditions, i.e. without flow, facilitated ion transfer,[20] interfacial pH control,[21] liquid|liquid electrocatalysis,[22] liquid|liquid extraction,[23] and biphasic electroluminescence[24] have been studied extensively. The boundary between the electrode and two liquid phases is called a three-phase junction. Kinetics and thermodynamics of electrochemical processes at such interfaces have been thoroughly investigated under stationary conditions.[25−38] For example, a methodology for determination of standard rate constants of ion and electron transfer reactions was developed.[25−28] Determination of standard Gibbs energy of transfer for a wide variety of ions, including simple organic[29−31] and inorganic anions,[32−35] alkali metal cations,[36] amino acids, and small peptides,[37,38] was also reported.

Under multiphase flow conditions, simultaneous reduction of hexaammineruthenium(III) chloride in the aqueous stream and oxidation of *N,N,N′,N′*-tetramethyl-1,4-phenylenediamine in 1,2-dichloroethane stream was studied by Fisher and co-workers.[16] Both the reduction and oxidation currents were proportional to the cube root of the flow rate.

In 2007, ion transfer processes driven by an electrode reaction of a redox probe were studied for the first time under microfluidic conditions by Marken and co-workers.[39] The authors investigated transfer of ClO_4^- anions across flowing *N*-octyl-2-pyrolidone (NOP)|water interface driven by electrooxidation of *n*-butylferrocene (*n*-BuFc). The *n*-BuFc oxidation current was shown to decrease with the flow rate. This was explained by the fact that ion transfer step that follows electrode reaction was hindered at higher flow rates. The ions

Received: September 18, 2013
Revised: November 12, 2013
Published: December 4, 2013

   dx.doi.org/10.1021/la403614z | *Langmuir* 2013, 29, 16034−16039

were simply washed through the channel, so they were not able to cross the interface. This suggested that a diffusion zone exists at the electrode|NOP|W three-phase junction.

Apart from the NOP|W biphasic system, electrochemistry in acetonitrile−water (ACN|W) microfluidic system was performed.[40,41] Microfluidic conditions revealed important differences between these two systems. While in the case of NOP|W the limiting current decreased with the flow rate, in the case of ACN|W the limiting current was independent of the flow rate. This has been explained by different mass transfer rates in these two organic solvents. Since ACN is less viscous than NOP, diffusion of *n*-BuFc through ACN to the three-phase junction is faster than diffusion of *n*-BuFc in NOP. Diffusion of *n*-BuFc in ACN is not hindered by the convective flow in the channel. In the case of the NOP|W system, *n*-BuFc is washed through the channel, and thus little material is able to reach the three-phase junction.

The aim of this work was to examine the effect of flow rate on the electrochemical behavior at a liquid|liquid interface over a wide range of flow rates. The flow rate is the easiest parameter to control under microfluidic conditions; hence, its effect on the electrochemical response must be determined and well understood as a first instance when dealing with electrochemistry in microfluidics. Our work was motivated by opposite observations made by aforementioned Fisher[16] and Marken[39−41] about the flow rate effect under multiphase flow conditions. Here, we attempted to provide a general explanation of the flow rate effect based on the two concurrent mass transport mechanisms: diffusion and convection. In this work, a novel electrochemical behavior at oil|water interface has been possible to be highlighted owing to the microfluidic conditions. We support our discussion with visualization of the interface by confocal microscopy. So far, oil|water interfaces have been visualized by confocal microscopy merely under stagnant conditions.[42,43] Under microfluidic conditions, only water|water[44] and air|water interfaces[45] have been visualized. We discuss for the first time the behavior of the flowing oil|water interface topography during an electrochemical process.

EXPERIMENTAL SECTION

Chemicals and Materials. The poly(dimethylsiloxane) (PDMS) elastomer and curing agent (Sylgard 184) for the microfluidic device were obtained from Dow Corning. Sodium perchlorate monohydrate (98%, Fluka), ferrocene (Fc) (98%, Aldrich), and *N*-octyl-2-pyrrolidone (NOP) (98%, Santa Cruz Biotechnolgy) were all used without further purification. AZ ECI 3027 positive photoresist, SU-8 negative photoresist, and AZ 400 K Developer were purchased from MicroChemicals GmbH. Rhodamine 101 inner salt as fluorescence dye in the aqueous phase was purchased from Sigma-Aldrich. Silicon wafers were obtained from Topsil. Filtered and demineralized water was taken from an ELIX purification system (Millipore).

Two-Phase Flow Microchip Design and Fabrication. The two-phase microfluidic channel was fabricated in PDMS using the replica micromolding method.[46] Photolithographic masters were prepared from SU-8 in base relief on silicon wafers and a PDMS/curing agent mixture (ratio 1:10) was poured onto the master and dried at 80 °C for 1.5 h. The system consists of a straight channel with Y-junctions for inlets and outlets for the aqueous and organic phases separately (Figure 1). The main channel has a width of 500 μm and height of 200 μm. Capillary channels (2 mm long and 50 μm wide) connect two side reservoirs with the main channel. In the reservoir on the aqueous side a 3 mm hole was punched out for placement of a Ag|AgCl|KCl_{3M} reference electrode (RE). The hole around the RE was sealed with a small amount of PDMS. The reservoir on the organic side is not used in these experiments but could house a second reference electrode for

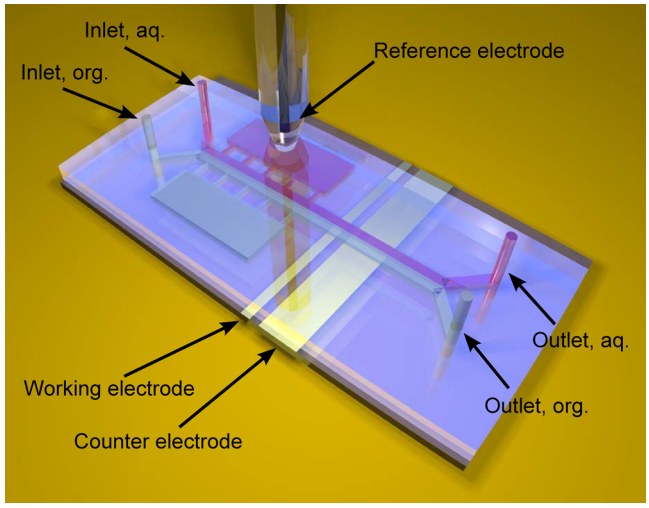

Figure 1. Schematic illustration of the two-phase microfluidic system.

using a four-electrode setup. Gold working and counter electrodes (width 1 and 5 mm, respectively) were patterned on a glass microscope slide using standard photolithography. The thickness of the sputtered gold electrodes were 150 nm with a 5 nm titanium adhesion layer. The PDMS channel was mounted to the glass plate with the electrodes perpendicular to the channel. The assembly was held together using a plexiglass holder. For the confocal microscopy measurements the PDMS was bonded to the glass plate by exposure to an O_2 plasma for 50 s (Harrick, Model PDC-32G-2, 100 W). To control the flow of the aqueous and organic phases, two synchronized syringe pumps (Harvard Apparatus, Pump 11 elite) were used. The syringes were connected to the channel using polyethylene tubing.

Electrochemistry and Microscopy. Cyclic voltammetry (CV) was conducted with an Autolab PgStat (Metrohm Autolab) electrochemical system. The working and counter electrodes were gold electrodes located in the bottom of the microfluidic channel. A silver−silver chloride electrode Ag|AgCl|KCl_{3M} was used as reference electrode placed in a side reservoir on the aqueous side of the channel.

During the electrochemical measurements the aqueous flow rate ($V_{f,aq}$) was kept 8 times higher than the organic flow rate ($V_{f,org}$) to keep the widths of the two parallel streams equal.[47]

We performed laser scanning confocal images using a commercially available NIKON A1-R system. The system is based on a motorized, NIKON TiE 2000 inverted microscope. The measurements were performed using a dry objective with ×10 magnification (NA 0.3, working distance 16 mm). The aqueous phase was stained with rhodamine 101 inner salt with a maximum of the absorption/emission at 560/589 nm. The wavelength of the diode laser used in experiments was equal to 561 nm. We made a cross section of the microfluidic channel using the 3D scanning mode of the confocal system. Separate focus planes were imaged at a frame rate of 1/8 fps. Four consecutive images were averaged to improve the signal-to-noise ratio. The distance between the focus planes was set to 5.175 μm.

RESULTS AND DISCUSSION

The dependence of the mass-transport-limited current of a redox reaction on the flow rate in a rectangular channel is given by the equation[1]

$$I_{lim} = 0.925nFcD^{2/3}(h^2d)^{-1/3}x^{2/3}wV_f^{1/3} \quad (1)$$

where n is the number of electrons transferred in the reaction, F is the Faraday constant, c is the concentration of the reacting species, D its diffusion constant, h the half-height and d the width of the channel, x the electrode length and w its width, and V_f the volume flow rate. This approximation is valid for a parabolic flow profile far from the side walls of the channel.

dx.doi.org/10.1021/la403614z | *Langmuir* 2013, 29, 16034−16039

However, the wall effect on the limiting current is usually quite small. Similarly, in very thin channels or at very low flow rates, the depletion layer above the electrode can reach the ceiling of the channel and affect the limiting current.[48] At the relatively high flow rates and thick channels used in this study, this effect can be ignored.

Here, we investigated the oxidation of Fc at the organic phaselaqueous phaselgold electrode triple phase junction. This is a well-known example of a coupled electron transfer−ion transfer process.[49,50] The organic phase was *N*-octyl-2-pyrrolidone without deliberately added supporting electrolyte and the aqueous phase contained 0.1 M $NaClO_4$ as supporting electrolyte. The overall reaction can be described by the equation

$$Fc(org) + ClO_4^-(aq) \rightleftharpoons Fc^+(org) + ClO_4^-(org) + e^- \quad (2)$$

In Figure 2, cyclic voltammograms of the oxidation of ferrocene at the three-phase junction can be seen. As was noted by

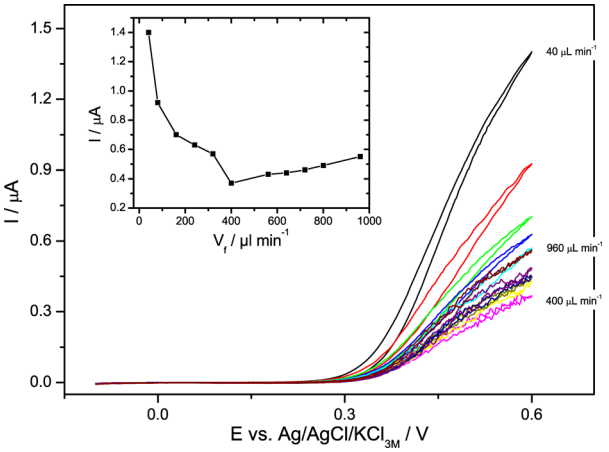

Figure 2. Cyclic voltammograms of the oxidation of 10 mM Fc in *N*-octyl-2-pyrrolidone at the NOP|0.1 M $NaClO_4$ in water|electrode junction. Aqueous flow rates 40, 80, 160, 240, 320, 400, 560, 640, 720, 800, and 960 μL min^{-1}. The inset shows the current at 0.6 V as a function of flow rate.

MacDonald and co-workers,[39] the current decreases as the flow rate is increased. This is in marked contrast to the standard behavior with $I_{lim} \propto V_f^{1/3}$ described by eq 1. This behavior was explained by the diffusion of ions into the organic phase, forming an extended reaction zone (see Figure 3). When the flow rate increases, the diffusion zone becomes narrower, which leads to a decrease in the current. However, at flow rates higher than those explored by the Marken group,[39−41] the current starts increasing. This change in behavior strongly suggests that two different mechanisms are at play.

We suggest that the decrease of the current can be attributed to the narrowing of the reaction zone while the eventual increase is an effect of the typical behavior. To test this we construct a simple model where the electrode width, w, in eq 1 is replaced by an effective reaction zone width, w_{eff}. Although liquidlliquid interfaces in principle can be thought of as molecularly sharp,[51] the situation is different at the three-phase junction where the contact with the solid phase disturbs the liquid junction which can e.g. lead to the formation of microemulsions.[52,53] In experiments with electrodeposition at three-phase junctions it has been shown that the narrowest structures that can be deposited are in the range of a few micrometers.[54,55] It is therefore reasonable to assume a minimal effective reaction zone width w_0 such that

$$w_{eff} = w_0 + w_{diff} \quad (3)$$

where the latter term is determined by diffusion of ions into the organic phase. How far ions have time to diffuse into the organic phase is determined by the speed of the liquid and thus by the flow rate. Keeping the ratio of $V_{f,org}$ to $V_{f,aq}$ constant allows the system to be described by a single flow rate V_f. As the diffusion width decreases with increasing flow rate, we can assume that $w_{diff} \propto V_f^{-\alpha}$, where α is a positive number. Since diffusion distance is proportional to the square root of the diffusion time,[1] a reasonable assumption would be that $\alpha = {}^1/_2$ such that $w_{diff} = w'_{diff}/V_f^{1/2}$. Replacing w in eq 1 with the expression in eq 3 gives a new equation of the form

$$I_{lim} = Zw_{eff}V_f^{1/3} = Zw_0V_f^{1/3} + Zw'_{diff}V_f^{-1/6} \quad (4)$$

Here $Z = 0.925nFcD^{2/3}(h^2d)^{-1/3}x^{2/3}$. We have fitted the data from Figure 2 to a function of the form $I_{lim} = AV_f^{1/3} + BV_f^{-1/6} + K$ (Figure 4). Identifying A and B with the constants from eq 4, we get a value of $w_0 = 21 \pm 7$ μm. The diffusion widens the effective electrode width to 100−200 μm over the relevant range of flow rates. Both of these values are reasonable,

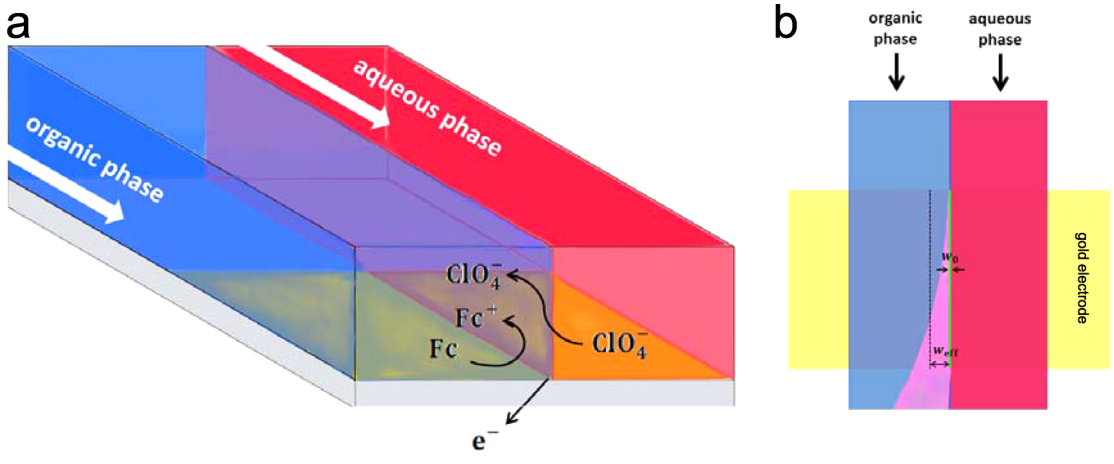

Figure 3. (a) Sketch of the flow system and the reaction at the three-phase junction. (b) Sketch of the proposed model of extended reaction zone.

dx.doi.org/10.1021/la403614z | *Langmuir* 2013, 29, 16034−16039

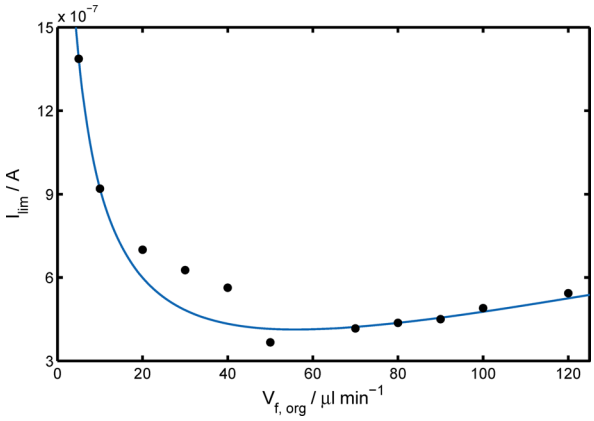

Figure 4. Oxidation current as a function of flow rate taken from Figure 2. The line is a fit to the data using the formula $I_{lim} = AV_f^{1/3} + BV_f^{-1/6} + K$ ($R^2 = 0.95$).

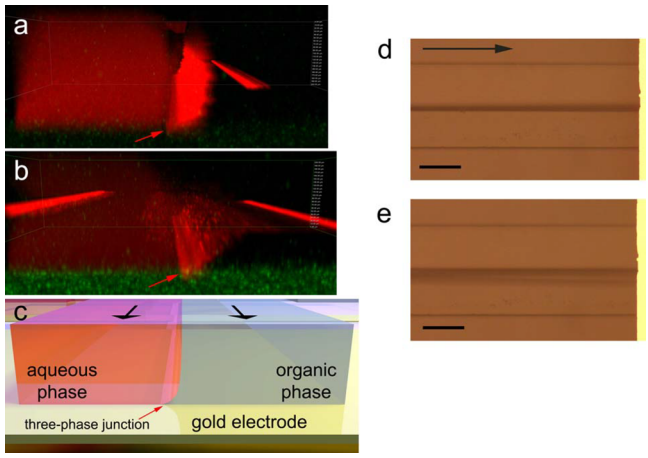

Figure 5. Laser scanning confocal fluorescent and light microscopy images of the liquidlliquid interface. The aqueous phase is marked by red fluorescence, the gold working electrode is green, and the organic phase is invisible. Parts a and b show confocal fluorescent images of the flow before the electrode at low ($V_{f,aq}$ = 160 μL min^{-1}) and high ($V_{f,aq}$ = 640 μL min^{-1}) flow rates, respectively. A potential of 0.6 V is applied to the electrode. In part c a schematic representation of the view in the confocal micrographs is shown. The red arrow shows the position of the three-phase junction. The full width of the channel is 500 μm and the height 200 μm. Parts d and e show the low and high flow rate regimes under a normal light microscope. The focus is on the upper part of the channel, and the blurring of the liquidlliquid junction is clearly seen. The aqueous phase is in the upper half of the image. The scale bar is 250 μm. The black arrows show the direction of the flow.

although the especially the latter is somewhat higher than expected. The likely reason is that the values were calculated using the flow rate to estimate the diffusion time. This gives the average speed of the liquid in the channel. Close to liquidlliquid junction the velocity of the organic phase is higher than the average since it is pulled along by the faster moving aqueous phase. This leads to a smaller value of w_{diff}. The values of w_0 and w_{diff} as well as the position of the current minimum changes somewhat from setup to setup, but the trend is always the same and the values stay within the reasonable range for the model.

To further investigate the system, we performed laser scanning confocal microscopy of the microchannel during operation with two immiscible liquids. For this purpose we used a microchannel where the PDMS was bonded to the glass slide by O_2-plasma treatment. However, the plasma treatment makes the glass slide extremely hydrophilic. The contact angle decreases from $CA_{aq} = 19 \pm 2°$ to only 2°. As a consequence, the aqueous phase completely covers the lower part of the channel with the organic phase squeezed into the upper corner. There is therefore no contact between the organic phase and bottom plate, and no three-phase junction is formed with the electrodes. This increased wetting of soda-lime glass is well-known.[56] Washing the channel with isopropanol after bonding returns the contact angle to its original value, and the behavior of the current matches that of the clamp-mounted channel. Neither the plasma treatment nor the subsequent cleaning with isopropanol affected the contact angle in a large degree between the glass and the NOP. After the cleaning the contact angle decreased slightly from $CA_{NOP} = 29 \pm 2°$ to $CA_{NOP} = 25 \pm 2°$.

Figure 5 shows cross section of the microchannel with the aqueous phase in red. The gold working electrode shows up as green due to reflection of the excitation laser. The liquidlliquid interface is marked by strong fluorescence because the dye partly adsorbs on the interface.[57] In the images at low flow rate (a, b) the liquidlliquid junction is clearly visible as a sharp edge, and the undercut of the organic phase under the aqueous phase, as described in the Marken papers,[39,41] is clearly visible. In contrast to the sharp edge at low flow rates the liquidlliquid interface at higher flow rates appears smeared with irregular fluorescence. A similar behavior can be seen under normal light microscope, without added dye, where the liquidlliquid junction seems to expand when the flow rate is increased beyond $V_{f,aq} \sim$ 400 μL min^{-1} (see Figure 5b,d). This is likely caused by the formation of an unstable flow or the formation of a microemulsion, despite the low Reynolds number even at these high flow rates. This behavior is also seen to a smaller degree at low flow rates at the very top of the channel. However, most importantly at the lower part of the channel the liquidlliquid junction is very stable both at low and high flow rates. This asymmetry can be attributed to the different wetting properties of the relatively hydrophilic glass surface and the hydrophobic PDMS where the difference in contact angle between water and NOP is much larger (CA_{aq} = 85°, CA_{NOP} = 45°). The stable three-phase junction means that, as described above, the change in current is probably due to extension of the reaction zone by ion diffusion as suggested by Marken et al.[41] and not because of the mixing of the phases. Furthermore, a small difference is seen in the curvature of the liquidlliquid junction close to the gold electrode if comparing images before and after the electrode (see Supporting Information). However, this difference is present also without application of a potential to the electrode and is therefore likely an effect of the different wetting properties of gold and glass. Thus, there is no significant effect of the reaction at the three-phase junction on the properties of the W|NOP interface. This is consistent with the transfer of only a small amount of ions into the organic phase.

■ CONCLUSIONS

We have investigated the ion transfer assisted oxidation of ferrocene at a flowing organic solvent|aqueous electrolyte| electrode triple phase junction in a microfluidic setup. Studies of the anomalous behavior of oxidation current as a function of flow rate reported by Marken and co-workers[39−41] was extended to higher flow rates and a reversal of the trend was observed. At low flow rates the current decreases with

dx.doi.org/10.1021/la403614z | Langmuir 2013, 29, 16034−16039

increasing V_f, in contrast to what is described by eq 1. However, at high flow rates the current increases and follows the expected $I_{lim} \propto V_f^{1/3}$ behavior. This was explained by a simple model assuming a minimum width of the three phase junction and a diffusion-controlled width inversely proportional to the square root of V_f.

We also investigated the liquid|liquid system using laser scanning confocal fluorescent microscopy. The fluorescent images clearly show the organic phase undercutting the aqueous phase. Importantly, we see a clear difference between the top and the bottom of the channel, where the liquid|liquid junction is quite sharp at the glass interface. In the upper part of the channel, close to the PDMS interface the two liquid phases seem to mix or form an emulsion. The likely reason for this is the almost equal wetting properties of the glass surface to the two liquids and the large difference in wetting angle for the PDMS|organic solvent and PDMS|aqueous electrolyte interfaces. However, the electrochemical measurements showed that a thin mixing zone exists also close to the liquid|liquid|glass interface, indicating that mixing might be an important effect to consider at all flowing liquid|liquid|solid interfaces. Also important is that no influence of the applied potential on the liquid|liquid junction topography was observed.

■ ASSOCIATED CONTENT

Supporting Information

Additional laser scanning fluorescent images of the liquid|liquid junction after the WE. This material is available free of charge via the Internet at http://pubs.acs.org.

■ AUTHOR INFORMATION

Corresponding Author

*E-mail martinj@ichf.edu.pl; Ph +48 22 343 3306; Fax +48 22 343 3333 (M.J.-N.).

Notes

The authors declare no competing financial interest.

■ ACKNOWLEDGMENTS

This work was financed by the Polish National Science Centre under contract 2011/01/D/ST4/04182 and partially supported by the European Union within the European Regional Development Fund, through the grant Innovative Economy (POIG.02.02.00-00-025/09). T.K. thanks the Polish National Science Centre for funding under the contract DEC1-2011/01/N/ST3/00865.

■ REFERENCES

(1) Brett, C. M. A.; Brett, A. M. O. *Electrochemistry: Principles, Methods, and Applications*; Oxford University Press: New York, 1993.

(2) Sun, X.; Gillis, K. D. On-chip amperometric measurement of quantal catecholamine release using transparent indium tin oxide electrodes. *Anal. Chem.* **2006**, *78*, 2521−2525.

(3) Song, H.; Chen, D. L.; Ismagilov, R. F. Reactions in droplets in microfluidic channels. *Angew. Chem., Int. Ed.* **2006**, *45*, 7336−7356.

(4) Shui, L.; Eijkel, J. C. T.; van den Berg, A. Multiphase flow in microfluidic systems -control and applications of droplets and interfaces. *Adv. Colloid Interface Sci.* **2007**, *133*, 35−49.

(5) Weibel, D. B.; Whitesides, G. M. Applications of microfluidics in chemical biology. *Curr. Opin. Chem. Biol.* **2006**, *10*, 584−591.

(6) Sia, S. K.; Whitesides, G. M. Microfluidic devices fabricated in poly(dimethylsiloxane) for biological studies. *Electrophoresis* **2003**, *24*.

(7) Wang, J. Electrochemical detection for microscale analytical systems: a review. *Talanta* **2002**, *56*, 223−231.

(8) Zimmerman, W. B. Electrochemical microfluidics. *Chem. Eng. Sci.* **2011**, *66*, 1412−1425.

(9) Jayashree, R. S.; Gancs, L.; Choban, E. R.; Primak, A.; Natarajan, D.; Markoski, L. J.; Kenis, P. J. a. Air-breathing laminar flow-based microfluidic fuel cell. *J. Am. Chem. Soc.* **2005**, *127*, 16758−16759.

(10) Kjeang, E.; Djilali, N.; Sinton, D. Microfluidic fuel cells: A review. *J. Power Sources* **2009**, *186*, 353−369.

(11) Swensen, J. S.; Xiao, Y.; Ferguson, B. S.; Lubin, A. a.; Lai, R. Y.; Heeger, A. J.; Plaxco, K. W.; Soh, H. T. Continuous, real-time monitoring of cocaine in undiluted blood serum via a microfluidic, electrochemical aptamer-based sensor. *J. Am. Chem. Soc.* **2009**, *131*, 4262−4266.

(12) Pumera, M.; Merkoçi, A.; Alegret, S. New materials for electrochemical sensing VII. Microfluidic chip platforms. *TrAC, Trends Anal. Chem.* **2006**, *25*, 219−235.

(13) Watts, P.; Haswell, S. J.; Pombo-Villar, E. Electrochemical effects related to synthesis in micro reactors operating under electrokinetic flow. *Chem. Eng. J.* **2004**, *101*, 237−240.

(14) Stalder, R.; Roth, G. P. Preparative microfluidic electrosynthesis of drug metabolites. *ACS Med. Chem. Lett.* **2013**, DOI: 10.1021/mL400316p.

(15) Wang, J.; Polsky, R.; Tian, B.; Chatrathi, M. Voltammetry on microfluidic chip platforms. *Anal. Chem.* **2000**, *72*, 5285−5289.

(16) Yunus, K.; Marks, C. B.; Fisher, A. C.; Allsopp, D. W. E.; Ryan, T. J.; Dryfe, R. A. W.; Hill, S. S.; Roberts, E. P. L.; Brennan, C. M. Hydrodynamic voltammetry in microreactors: multiphase flow. *Electrochem. Commun.* **2002**, *4*, 579−583.

(17) Fisher, A. C.; Gooch, K. A.; Henley, I. E.; Yunus, K. Voltammetry under microfluidic control. *Anal. Sci.* **2001**, *17*, i371−i374.

(18) Sinkala, E.; McCutcheon, J. E.; Schuck, M. J.; Schmidt, E.; Roitman, M. F.; Eddington, D. T. Electrode calibration with a microfluidic flow cell for fast-scan cyclic voltammetry. *Lab Chip* **2012**, *12*, 2403−2408.

(19) Gu, Y.; Fisher, A. C. An ac voltammetry approach for the detection of droplets in microfluidic devices. *Analyst* **2013**, *138*, 4448−52.

(20) Katif, N.; Harries, R. A.; Kelly, A. M.; Fossey, J. S.; James, T. D.; Marken, F. Boronic acid-facilitated α-hydroxy-carboxylate anion transfer at liquid/liquid electrode systems: the EICrev mechanism. *J. Solid State Electrochem.* **2008**, *13*, 1475−1482.

(21) Kelly, A. M.; Katif, N.; James, T. D.; Marken, F. N,N-Butyl-decamethylferrocenyl-amine reactivity at liquid |liquid interfaces: electrochemically driven anion transfer vs. pH driven proton transfer. *New J. Chem.* **2010**, *34*, 1261.

(22) Katif, N.; MacDonald, S.; Kelly, A.; Galbraith, E.; James, T.; Lubben, A.; Opallo, M.; Marken, F. Electrocatalytic determination of sulfite at immobilized microdroplet liquid| liquid interfaces: The EIC' mechanism. *Electroanalysis* **2008**, *20*, 469−475.

(23) Reyna-González, J. M.; Torriero, A. A. J.; Siriwardana, A. I.; Burgar, I. M.; Bond, A. M. Extraction of copper(II) ions from aqueous solutions with a methimazole-based ionic liquid. *Anal. Chem.* **2010**, *82*, 7691−8.

(24) Lledo-Fernandéz, C.; Hatay, I.; Ball, M. J.; Greenway, G. M.; Wadhawan, J. Electrogenerated chemiluminescence at droplet-modified electrodes: towards biphasic pK_a measurement via proton-coupled electron transfer at liquid| liquid interfaces. *New J. Chem.* **2009**, *33*, 749.

(25) Quentel, F.; Mirčeski, V.; Elleouet, C.; L'Her, M. Studying the thermodynamics and kinetics of ion transfers across water-2-nitrophenyloctyl ether interface by means of organic-solution-modified electrodes. *J. Phys. Chem. C* **2008**, *112*, 15553−15561.

(26) Quentel, F.; Mirčeski, V.; L'Her, M. Kinetics of anion transfer across the liquid| liquid interface of a thin organic film modified electrode, studied by means of square-wave voltammetry. *Anal. Chem.* **2005**, *77*, 1940−1949.

(27) Gulaboski, R.; Mirčeski, V.; Pereira, C. M.; Cordeiro, M. N. D. S.; Silva, A. F.; Quentel, F.; L'Her, M.; Lovrić, M. A comparative study of the anion transfer kinetics across a water/nitrobenzene interface by

means of electrochemical impedance spectroscopy and square-wave voltammetry at thin organic film-modified electrodes. *Langmuir* **2006**, *22*, 3404−3412.
(28) Mirčeski, V.; Quentel, F.; L'Her, M.; Pondaven, A. Studying the kinetics of the ion transfer across the liquidl liquid interface by means of thin film-modified electrodes. *Electrochem. Commun.* **2005**, *7*, 1122−1128.
(29) Gulaboski, R.; Mirčeski, V.; Scholz, F. An electrochemical method for determination of the standard Gibbs energy of anion transfer between water and n-octanol. *Electrochem. Commun.* **2002**, *4*, 277−283.
(30) Komorsky-Lovrić, S.; Riedl, K.; Gulaboski, R.; Mirčeski, V.; Scholz, F. Determination of standard Gibbs energies of transfer of organic anions across the water/nitrobenzene interface. *Langmuir* **2003**, *19*, 3090−3090.
(31) Komorsky-Lovrić, S.; Riedl, K.; Gulaboski, R.; Mirčeski, V.; Scholz, F. Determination of standard Gibbs energies of transfer of organic anions across the water/nitrobenzene interface. *Langmuir* **2002**, *18*, 8000−8005.
(32) Bouchard, G.; Galland, A.; Carrupt, P.-A.; Gulaboski, R.; Mirčeski, V.; Scholz, F.; Girault, H. H. Standard partition coefficients of anionic drugs in the n-octanol/water system determined by voltammetry at three-phase electrodes. *Phys. Chem. Chem. Phys.* **2003**, *5*, 3748.
(33) Scholz, F.; Komorsky-Lovrić, S.; Lovrić, M. A new access to Gibbs energies of transfer of ions across liquidl liquid interfaces and a new method to study electrochemical processes at well-defined three-phase junctions. *Electrochem. Commun.* **2000**, *2*, 112−118.
(34) Gulaboski, R.; Riedl, K.; Scholz, F. Standard Gibbs energies of transfer of halogenate and pseudohalogenate ions, halogen substituted acetates, and cycloalkyl carboxylate anions at the waterl nitrobenzene interface. *Phys. Chem. Chem. Phys.* **2003**, *5*, 1284−1289.
(35) Mirčeski, V.; Gulaboski, R.; Scholz, F. Determination of the standard Gibbs energies of transfer of cations across the nitrobenzenel water interface utilizing the reduction of iodine in an immobilized nitrobenzene droplet. *Electrochem. Commun.* **2002**, *4*, 814−819.
(36) Scholz, F.; Gulaboski, R.; Caban, K. The determination of standard Gibbs energies of transfer of cations across the nitrobenzenel water interface using a three-phase electrode. *Electrochem. Commun.* **2003**, *5*, 929−934.
(37) Gulaboski, R.; Mirčeski, V.; Scholz, F. Determination of the standard Gibbs energies of transfer of cations and anions of amino acids and small peptides across the water nitrobenzene interface. *Amino Acids* **2003**, *24*, 149−54.
(38) Gulaboski, R.; Scholz, F. Lipophilicity of peptide anions: An experimental data set for lipophilicity calculations. *J. Phys. Chem. B* **2003**, *107*, 5650−5657.
(39) MacDonald, S. M.; Watkins, J. D.; Gu, Y.; Yunus, K.; Fisher, A. C.; Shul, G.; Opallo, M.; Marken, F. Electrochemical processes at a flowing organic solventl electrolyte phase boundary. *Electrochem. Commun.* **2007**, *9*, 2105−2110.
(40) Watkins, J. D.; MacDonald, S. M.; Fordred, P. S.; Bull, S. D.; Gu, Y.; Yunus, K.; Fisher, A. C.; Bulman-Page, P. C.; Marken, F. High-yield acetonitrile | water triple phase boundary electrolysis at platinised Teflon electrodes. *Electrochim. Acta* **2009**, *54*, 6908−6912.
(41) MacDonald, S. M.; Watkins, J. D.; Bull, S. D.; Davies, I. R.; Gu, Y.; Yunus, K.; Fisher, A. C.; Bulman Page, P. C.; Chan, Y.; Elliott, C.; Marken, F. Two-phase flow electrosynthesis: Comparing N-octyl-2-pyrrolidone-aqueous and acetonitrile-aqueous three-phase boundary reactions. *J. Phys. Org. Chem.* **2008**, *22*, 52−58.
(42) Dale, S. E.; Unwin, P. R. Polarised liquid/liquid micro-interfaces move during charge transfer. *Electrochem. Commun.* **2008**, *10*, 723−726.
(43) Kitazumi, Y.; Kakiuchi, T. Imaging of the liquid-liquid interface under electrochemical instability using confocal fluorescence microscopy. *Langmuir* **2009**, *25*, 10829−10833.
(44) Yamaguchi, Y.; Takagi, F.; Watari, T.; Yamashita, K.; Nakamura, H.; Shimizu, H.; Maeda, H. Interface configuration of the two layered laminar flow in a curved microchannel. *Chem. Eng. J.* **2004**, *101*, 367−372.
(45) Huh, D.; Tung, Y.-C.; Wei, H.-H.; Grotberg, J. B.; Skerlos, S. J.; Kurabayashi, K.; Takayama, S. Use of air-liquid two-phase flow in hydrophobic microfluidic channels for disposable flow cytometers. *Biomed. Microdevices* **2002**, *4*, 141−149.
(46) Mcdonald, J. C.; Duffy, D. C.; Anderson, J. R.; Chiu, D. T.; Wu, H.; Schueller, O. J. A.; Whitesides, G. M. Fabrication of microfluidic systems in poly(dimethylsiloxane). *Electrophoresis* **2000**, *21*, 27−40.
(47) The ratio of the width of the streams is given by $w_{aq}/w_{org} = \eta_{aq}/\eta_{org} \times V_{faq}/V_{forg}$. At 20 °C the viscosity of NOP is approximately 8 times that of water (8×10^{-3} and 1×10^{-3} Pa s, respectively).
(48) Amatore, C.; Da Mota, N.; Sella, C.; Thouin, L. Theory and experiments of transport at channel microband electrodes under laminar flows. 1. Steady-state regimes at a single electrode. *Anal. Chem.* **2007**, *79*, 8502−8510.
(49) Shul, G.; Opallo, M. Ceramic carbon electrode modified with redox probe and salt solution in hydrophobic polar solvent. *Pol. J. Chem.* **2004**, *78*, 1449−1456.
(50) Scholz, F.; Gulaboski, R. Determining the Gibbs energy of ion transfer across water-organic liquid interfaces with three-phase electrodes. *ChemPhysChem* **2005**, *6*, 16−28.
(51) Ilan, B. Theoretical study of the water/1,2-dichloroethane interface: Structure, dynamics, and conformational equilibria at the liquid−liquid interface. *J. Phys. Chem.* **1992**, *97*, 1432−1445.
(52) Aoki, K.; Li, M.; Chen, J.; Nishiumi, T. Spontaneous emulsification at oil-water interface by tetraalkylammonium chloride. *Electrochem. Commun.* **2009**, *11*, 239−241.
(53) Kaminska, I.; Jonsson-Niedziolka, M.; Kaminska, A.; Pisarek, M.; Hołyst, R.; Opallo, M.; Niedziolka-Jonsson, J. Electrodeposition of well-adhered multifarious Au particles at a solidltoluenelaqueous electrolyte three-phase junction. *J. Phys. Chem. C* **2012**, *116*, 22476−22485.
(54) Davies, T. J.; Wilkins, S. J.; Compton, R. G. The electrochemistry of redox systems within immobilised water droplets. *J. Electroanal. Chem.* **2006**, *586*, 260−275.
(55) Niedziolka, J.; Opallo, M. Electrochemically assisted sol-gel process at a three phase junction. *Electrochem. Commun.* **2008**, *10*, 1445−1447.
(56) DeRosa, R. L.; Schader, P. A.; Shelby, J. E. Hydrophilic nature of silicate glass surfaces as a function of exposure condition. *J. Non-Cryst. Solids* **2003**, *331*, 32−40.
(57) Ishizaka, S.; Nakatani, K.; Habuchi, S.; Kitamura, N. Total internal reflection fluorescence dynamic anisotropy of sulforhodamine 101 at a liquid/liquid interface: Rotational reorientation times and interfacial structures. *Anal. Chem.* **1999**, *71*, 419−426.